Molecular Immunology 111 (2019) 1–10

Contents lists available at ScienceDirect

Molecular Immunology

journal homepage: www.elsevier.com/locate/molimm

Ventilator-induced lung injury is alleviated by inhibiting NLRP3 inflammasome activation

Huan Liu, Changping Gu, Mengjie Liu, Ge Liu, Dong Wang, Xiaobin Liu, Yuelan Wang*

Department of Anesthesiology and Perioperative Medicine, Shandong Provincial Qianfoshan Hospital, Shandong University, No. 16766 Jingshi Road, Jinan, 250014, Shandong Province, China

ARTICLE INFO

Keywords:
NLRP3 inflammasome
Ventilator-induced lung injury
Cyclic stretch
Mechanical ventilation
Junction proteins
Inflammation

ABSTRACT

Background: Mechanical ventilation (MV) is frequently used but can aggravate or cause lung injury, known as ventilator-induced lung injury (VILI). However, the mechanisms are unclear. The NLR family pyrin domain containing 3 (NLRP3) inflammasome is a vital component of innate immunity and is closely related to VILI.
Methods: Mouse lung epithelial (MLE-12) cells were transfected with NLRP3 small interfering RNA (siRNA) or scramble siRNA (sc siRNA) and subjected to 20% cyclic stretch (CS). Wild-type C57BL/6 mice were injected with a liquid complex of NLRP3 siRNA/sc siRNA-Lipofectamine 2000 through the fundus venous plexus before mechanical ventilation. Western blots, immunoprecipitation, ELISAs, flow cytometry, immunofluorescence, and hematoxylin-eosin staining were used to assess the effects of the NLRP3 inflammasome on VILI and the mechanisms of those effects.
Results: CS activated the NLRP3 inflammasome by activating NIMA-related kinase 7 (NEK7). NLRP3 depletion inhibited NLRP3 inflammasome activation; alleviated the degradation of cell junction proteins, including p120-catenin (p120) and occludin; ameliorated the colocalization of p120 and E-cadherin; and mitigated the decrease in mitochondrial membrane potential caused by mechanical stretch. Furthermore, after NLRP3 depletion, VILI was attenuated by decreasing IL-1β secretion and pulmonary edema.
Conclusions: Inhibiting NLRP3 inflammasome activation ameliorated VILI, suggesting a potential therapeutic target for the clinical treatment of VILI.

1. Introduction

Mechanical ventilation can maintain airway patency, ameliorate oxygenation disorders and prevent hypoxia and carbon dioxide accumulation (Seiberlich et al., 2011). Mechanical ventilation has been widely used for patients with acute lung injury (ALI) or acute respiratory distress syndrome (ARDS) (Lewandowski, 1999; Blank and Napolitano, 2011; Yadam et al., 2016). However, this treatment can also cause ventilator-induced lung injury (VILI), which increases the morbidity and mortality of patients receiving ventilator therapy (Gattinoni et al., 2016; Kuipers et al., 2012; Hess et al., 2003).

Analysis of the mechanisms of VILI has indicated that this process involves barotrauma, volutrauma, atelectrauma and biotrauma (Jain et al., 2017; Keszler, 2005; Gudmundsson et al., 2018; Cannizzaro et al., 2011), pulmonary inflammatory responses induced by mechanical ventilation via recruitment of inflammatory cells and activation and release of inflammatory mediators and cytokines (Xi et al., 2016; Hoffman and Wanderer, 2010). Lung injury eventually occurs due to an imbalance between proinflammatory and anti-inflammatory mediators. In addition, mechanical ventilation induces alveolar membrane dysfunction and increases the permeability of the pulmonary vasculature, leading to pulmonary edema, which is primarily caused by the degradation of cell junction proteins (Gu et al., 2015). However, these changes are inseparable from the downstream effects of NLRP3 inflammasome activation.

The NLRP3 inflammasome is a cytoplasmically expressed pattern-recognition receptor that consists of NLRP3, apoptosis-associated speck-like protein (ASC) and caspase-1 and is classified among the NOD-like receptors, a family of proteins containing nucleotide-binding oligomers (Xu et al., 2012; Gov et al., 2017). The activated NLRP3 inflammasome can recognize many types of pathogens and dangerous molecules and participate in the immune response, ultimately causing various metabolic or immune diseases (Lee et al., 2016). Nigericin, ATP, lipopolysaccharide (LPS) or uric acid crystals cause NLRP3 to bind to the adaptor protein ASC via a homotypic interaction of PYD domains (Han et al., 2015; Gasse et al., 2009; Babelova et al., 2009), and ASC is then

* Corresponding author.
E-mail address: junzhustory@sina.com (Y. Wang).

https://doi.org/10.1016/j.molimm.2019.03.011
Received 23 January 2019; Received in revised form 28 February 2019; Accepted 26 March 2019
Available online 02 April 2019
0161-5890/

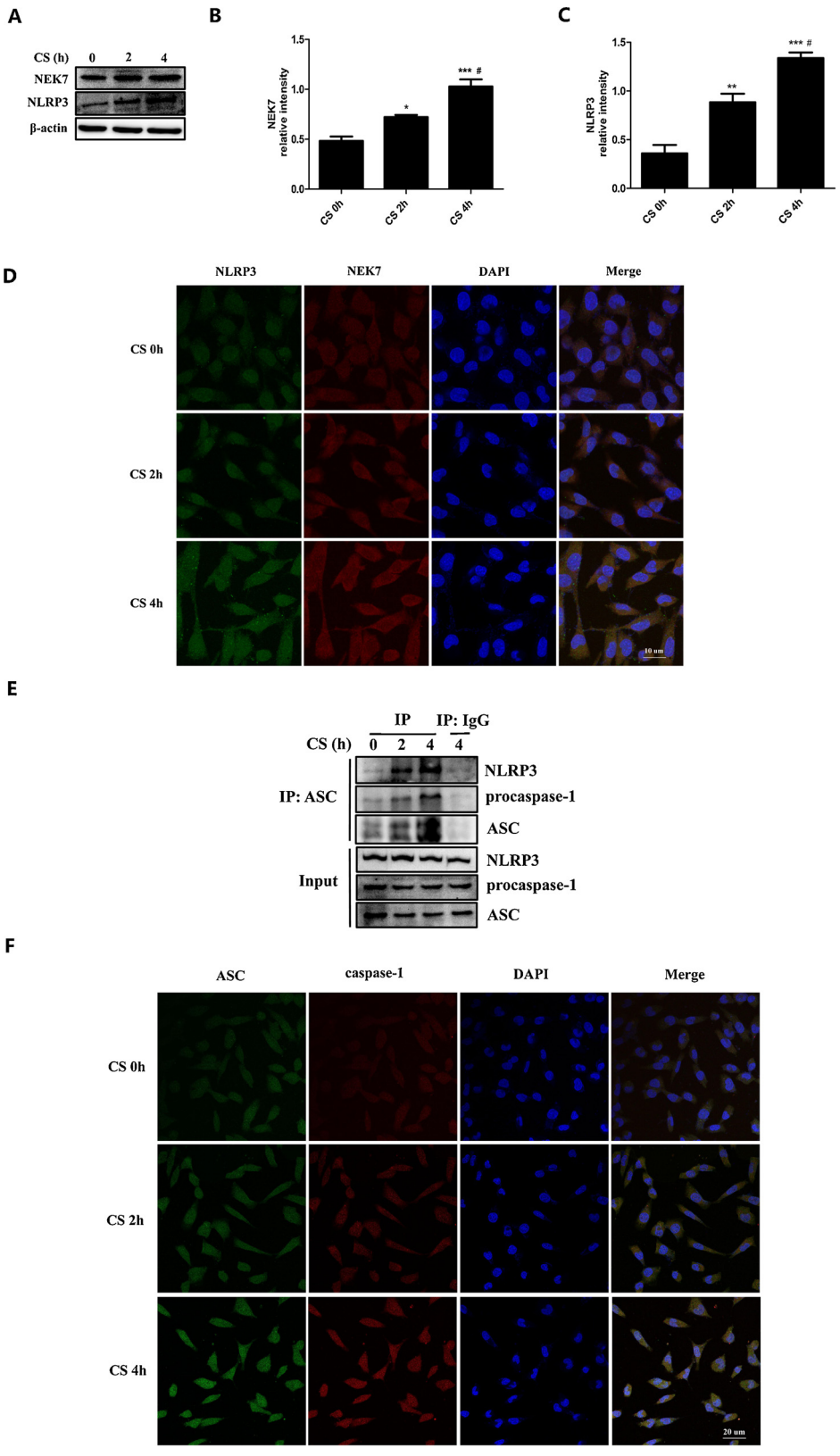

Fig. 1. Cyclic stretch induced NLRP3 inflammasome activation by activating NEK7. **(A)** The protein levels of NLRP3 and NEK7 were measured by Western blotting. **(B–C)** $^{*}p < 0.05$, $^{***}p < 0.001$, and $^{**}p < 0.01$ versus the control group. $^{\#}p < 0.05$ versus the CS 2 h group. **(D)** Immunofluorescence was used to analyze the colocalization of NLRP3 (green) and NEK7 (red), and the nuclei were stained with DAPI (blue). The scale bar was 10 μm. **(E)** The combination of NLRP3, ASC, and procaspase-1 was detected by immunoprecipitation after cyclic stretch for 0, 2, and 4 h. **(F)** The colocalization of ASC and caspase-1 was detected by immunofluorescence. MLE-12 cells were incubated with a mixture of anti-ASC and anti-caspase-1 antibodies, followed by IFKine donkey anti-mouse IgG (green) and IFKine donkey anti-rabbit IgG (red). The nuclei were stained with DAPI (blue). The scale bar was 20 μm. All experiments were repeated at least three times (For interpretation of the references to colour in this figure legend, the reader is referred to the web version of this article).

oligomerized, which recruits procaspase-1 in its mature form. Eventually, pro-IL-1β and pro-IL-18 are processed into their biologically active forms, resulting in lung injury. Previous studies have found that activation of the NLRP3 inflammasome occurs in two ways: the NLRP3 inflammasome can be activated after TLR-4/NF-κB pathway activation, or microbe- or risk-associated molecular patterns can activate the inflammasome directly (Wu et al., 2013).

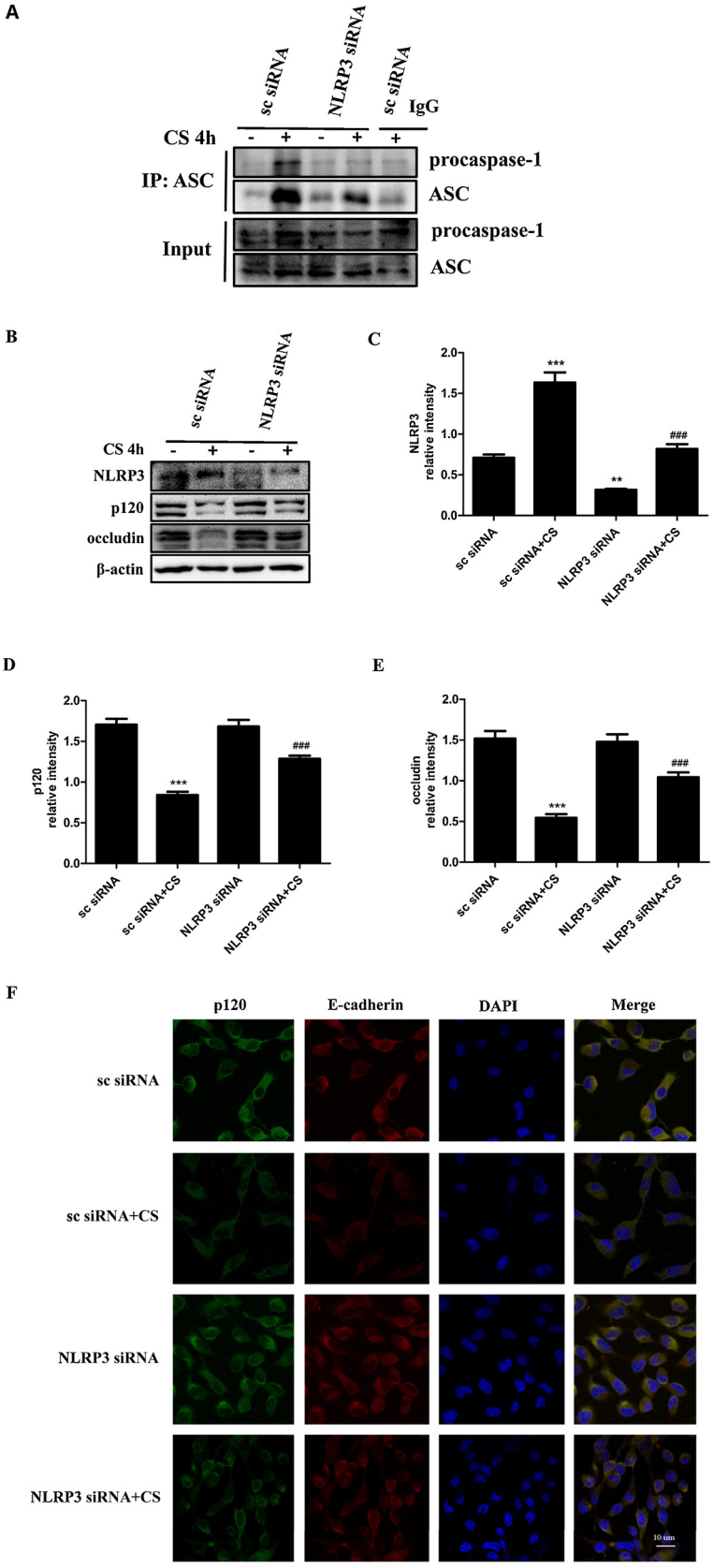

Fig. 2. NLRP3 regulated NLRP3 inflammasome activation and the degradation of cell junction proteins after cyclic stretching. (A) The combination of ASC and procaspase-1 was detected by immunoprecipitation in the NLRP3 siRNA- or sc siRNA-treated groups after cyclic stretching. **(B)** Western blotting was used to determine the expression of NLRP3, p120 and occludin. β-actin was used as a reference. **(C–E)** Statistical analysis of the relative density of the bands is displayed. All experiments were repeated at least three times. $^{***}p < 0.001$, $^{**}p <$ 0.01 versus the sc siRNA group. $^{\#\#\#}p < 0.001$ versus the sc siRNA + CS group. **(F)** Immunofluorescence was used to detect the colocalization of p120 and E-cadherin. MLE-12 cells were transfected with NLRP3 siRNA or sc siRNA before cyclic stretch and then incubated with a mixture of anti-p120 and anti-E-cadherin antibodies, followed by IFKine donkey anti-mouse lgG (green) and DyLight 594 goat anti-rat IgG (red). The nuclei were stained with DAPI (blue). The scale bar was 10 μm (For interpretation of the references to colour in this figure legend, the reader is referred to the web version of this article).

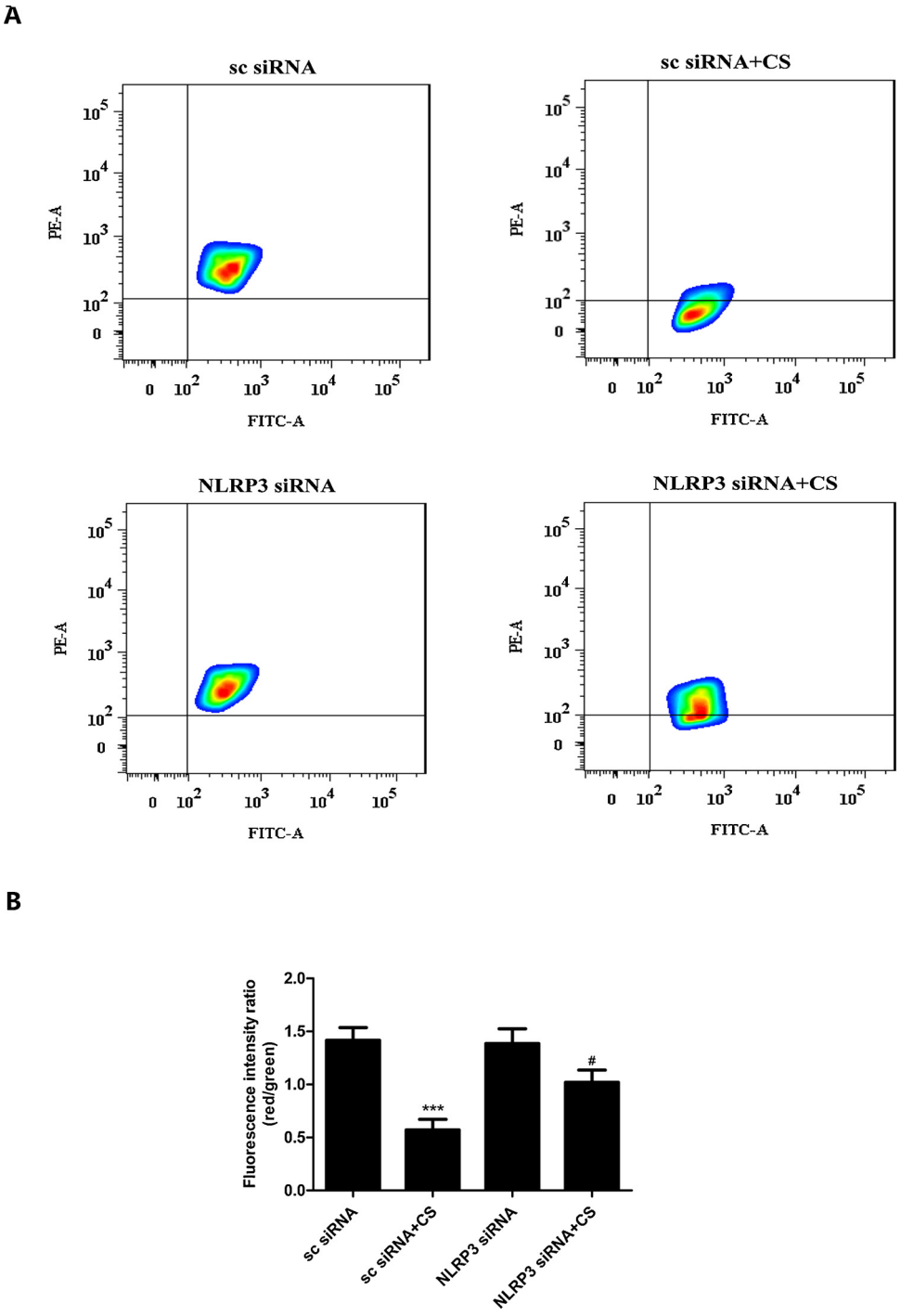

Fig. 3. NLRP3 mediated the changes in mitochondrial membrane potential caused by cyclic stretching. Fluorescence intensity ratio of red/green were used to measure the changes in mitochondrial membrane potential. All the experiments were repeated at least three times. $^{***}p < 0.001$ versus the sc siRNA group, $^{\#}p < 0.05$ versus the sc siRNA + CS group (For interpretation of the references to colour in this figure legend, the reader is referred to the web version of this article).

2. Materials and methods

2.1. Cell culture, NLRP3 knockdown in MLE-12 cells and cyclic stretch

MLE-12 cells were purchased from the American Type Culture Collection (Manassas, VA). The cells were seeded on collagen I-coated flexible-bottom BioFlex plates in Dulbecco's modified Eagle's medium with 10% fetal bovine serum and cultured for 10 h in a cell incubator at 37 °C with 5% CO_2. NLRP3 siRNA and sc siRNA (Santa Cruz, USA) were transfected into 70% confluent MLE-12 cells with Lipofectamine 2000 transfection reagent (Invitrogen, USA). After 48 h, confluent MLE-12 cells were starved for an hour prior to cyclic stretch using the FX-5000 T Flexercell Tension Plus system (Flexcell International, McKeesport, PA) with 20% stretch amplitude at a frequency of 30 cycles/min (0.5 Hz) and a stretch-to-relaxation ratio of 1:1 applied in a cyclic manner (Wang et al., 2011; Zhao et al., 2014). Unstretched cells in ordinary 6-well plates were used as the control group. MLE-12 cells were divided into four groups: (i) sc siRNA, (ii) sc siRNA + CS, (iii) NLRP3 siRNA, and (iv) NLRP3 siRNA + CS. All subsequent experiments were conducted after cyclic stretching, and the transfection was verified by Western blot analyses.

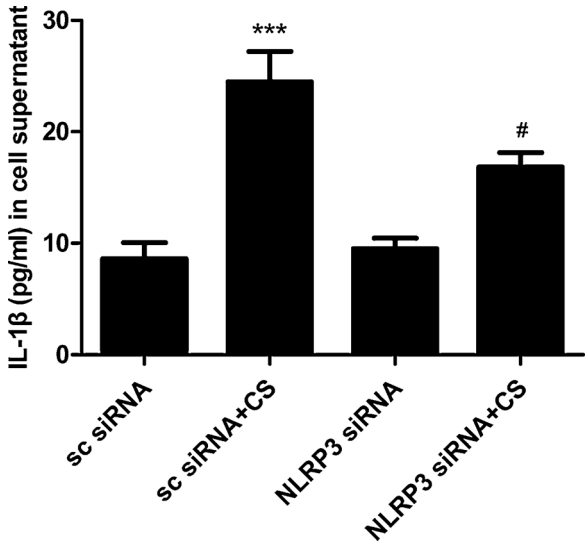

Fig. 4. Role of NLRP3 in regulating the secretion of IL-1β induced by cyclic stretching. The levels of IL-1β in cell supernatant were detected by ELISAs. All the experiments were repeated at least three times. $^{***}p < 0.001$ versus the sc siRNA group, $^{\#}p < 0.05$ versus the sc siRNA + CS group.

2.2. Flow cytometry assays

After cyclic stretching for 4 h, the cell supernatant was collected for ELISAs, and the confluent MLE-12 cells were washed twice with phosphate buffer solution (PBS). The cells were then cultured with trypsin-EDTA solution for 2 min. Subsequently, the cell suspension was placed in 1.5 ml Eppendorf tubes and centrifuged at 1200 rpm at 4 °C for 5 min to pellet the detached cells. Then, the detached cells were washed with PBS. Jc-1 staining solution (1 ml) was added to the sedimentation to incubate for 20 min at 37 °C. Then, the extracellular solution was removed after centrifuging at 1200 rpm at 4 °C for 5 min, and the cells were washed twice with 1 ml Jc-1 staining buffer. Finally, 500 μl Jc-1 staining buffer was added to resuspend the detached cells. Flow cytometry was used to analyze the changes in mitochondrial membrane potential (Zhang et al., 2017).

2.3. Animals

Wild-type male C57BL/6 mice (n = 80, 8–10 weeks of age, 25–30 g) were obtained from Vital River Laboratory (Beijing, China) and housed under specific pathogen-free conditions. The experiments were approved by the Animal Ethics Committee of Qianfoshan Hospital of Shandong University. A liquid complex of NLRP3 siRNA/sc siRNA-Lipofectamine 2000 was injected into each mouse twice a week through the fundus venous plexus in a solution of 125 μl NLRP3 siRNA/sc siRNA (40 μM) (GenePharma, China) and 12 μl Lipofectamine 2000 diluted in 100 μl diethyl pyrocarbonate (DEPC)-treated water. Mice were randomly divided into the following four groups, with 20 in each group: (i) sc siRNA: tracheal intubation without mechanical ventilation; (ii) sc siRNA + MV: tracheal intubation with 4 h of mechanical ventilation; (iii) NLRP3 siRNA: NLRP3 siRNA treatment with tracheal intubation without mechanical ventilation; (iv) NLRP3 siRNA + MV: NLRP3 siRNA treatment with tracheal intubation and mechanical ventilation for 4 h.

2.4. Hematoxylin-eosin (H-E) staining and lung injury scores

Briefly, lung tissues were fixed in formalin and embedded with paraffin and then sectioned into 5 μm slices. The H-E-stained sections were observed under a light microscope at a magnification of 400×.

To visually describe the pathological changes among the four groups, we evaluated the changes according to criteria based on previous studies. The degree of lung injury was scored based on pulmonary edema, destroyed pulmonary architecture, thickened alveolar septa, hyaline membrane formation, alveolar hemorrhage and infiltration of inflammatory cells, and at least three visual fields were observed for each slice. We adopted a scale of 0–4 to describe the severity of the lung injury: 0 represents no damage, 1 represents mild damage, 2 represents moderate damage, 3 represents severe damage and 4 represents very serious damage (Zhao et al., 2014; Liu et al., 2017).

2.5. Bronchoalveolar lavage fluid (BALF) and blood sampling

After 4 h of mechanical ventilation, bronchoalveolar lavage was performed in the four groups. With three 1 ml disposable syringes, 0.3 ml precooled saline was injected into the lungs of the mice by tracheal intubation and then pumped back after three seconds. The same operation was repeated three times, and the recovery rate was 90%.

Eppendorf tubes and 1 ml disposable syringes were heparinized prior to blood sampling from the abdominal aorta, and plasma was collected after centrifugation for 10 min at 3000 rpm and 4 °C.

2.6. Lung wet/dry (W/D) weight ratio

After mechanical ventilation, we injected heparin through the postcava and then rapidly collected the lung tissues. Filter paper was used to drain the surface blood from the lung tissues, which were then placed on an electronic balance to determine the wet lung weight. The lung tissues were dried at 65 °C for 48 h and weighed again to determine the dry weight; finally, the lung W/D ratio was calculated.

2.7. ELISA

The IL-1β levels in the cell supernatant, BALF and plasma were detected by ELISA according to the procedures in the kits (Elabscience, China).

2.8. Western blotting and immunoprecipitation

MLE-12 cells and lung tissues were lysed on ice in a mixture of RIPA and PMSF (Beyotime, China). The protein concentration was measured using a bicinchoninic acid (BCA) protein estimation kit (Beyotime, China). Equal amounts of protein were separated by 10% SDS-PAGE, after which, the proteins were transferred to polyvinylidene fluoride membranes. The membranes were blocked in 5% nonfat milk for 2 h at room temperature before being incubated with primary antibodies at 4 °C overnight. The primary antibodies were as follows: NEK7 (1:200) (Santa Cruz, USA), NLRP3 (1:500) (Cell Signaling Technology, USA), ASC (1:200) (Santa Cruz, USA), caspase-1 (1:200) (Santa Cruz, USA), p120 (1:5000) (Abcam, UK), occludin (1:2000) (Abcam, UK) and β-actin (1:1000) (Cell Signaling Technology, USA). The membranes were washed thrice with 20% Tween in TBS before being incubated with goat anti-mouse or goat anti-rabbit secondary antibodies for 2 h at room temperature. After the samples were washed with TBST, ECL SuperSignal reagent (Millipore, USA) was used to detect the protein bands. ImageJ software was used to analyze the relative densities of the proteins.

Immunoprecipitation was performed after MLE-12 cells were stimulated by cyclic stretching. Cells were lysed in buffer with a protease cocktail for 30 min; one part of the supernatant was used for input, and the other part was precleared using isotype control IgG together with 20 μl protein A/G plus-agarose beads for 4 h before incubation with anti-ASC antibody together with 20 μl protein A/G plus-agarose beads at 4 °C overnight. Finally, the immunoprecipitated proteins were dissolved in 2× loading buffer for immunoblot analysis.

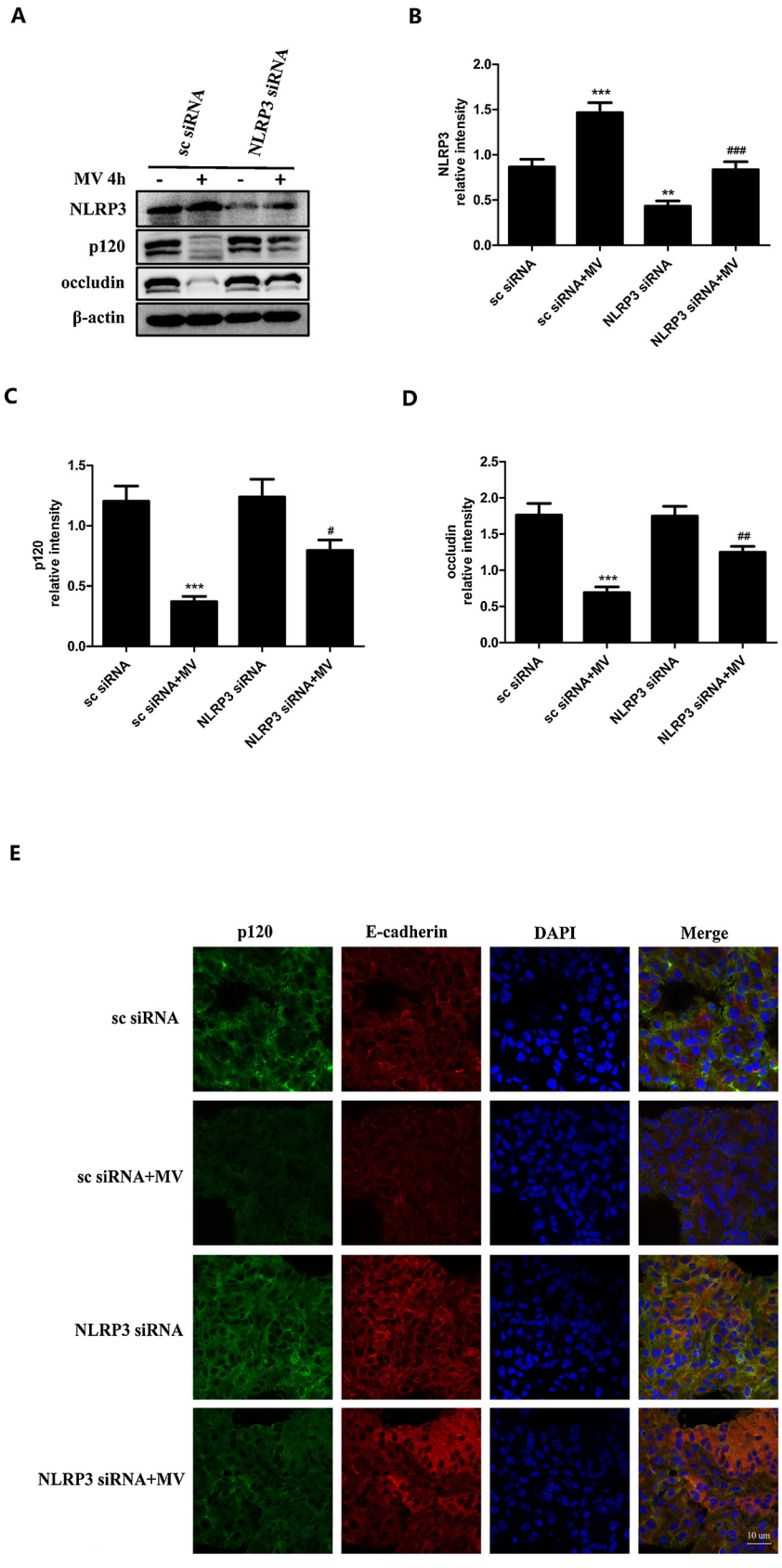

Fig. 5. NLRP3 mediated the degradation of cell junction proteins after mechanical ventilation. (A) The expression of NLRP3, p120 and occludin were determined by Western blotting, β-actin was used as a reference. **(B–D)** The relative density analysis of them were shown like that. $^{***}p < 0.001$, $^{**}p < 0.01$ versus the sc siRNA group. $^{###}p < 0.001$, $^{#}p < 0.05$, $^{##}p < 0.01$ versus the sc siRNA + MV group. **(E)** The colocalization of p120 (green) and E-cadherin (red) in lung tissues was determined by immunofluorescence, the nuclei were stained with DAPI (blue). The scale bar was 10 μm, we all did at least three independent repeated experiments (For interpretation of the references to colour in this figure legend, the reader is referred to the web version of this article).

2.9. Immunofluorescence

After processing, MLE-12 cells and frozen sections were fixed with 4% paraformaldehyde for 20 min and permeabilized with 0.5% Triton X-100 for 5 min, but the membrane proteins did not require this step. Then, the specimens were blocked with 5% BSA for 30 min at room temperature. The flexible membranes were trimmed, and slides with cells were collected. These samples were eventually placed on glass

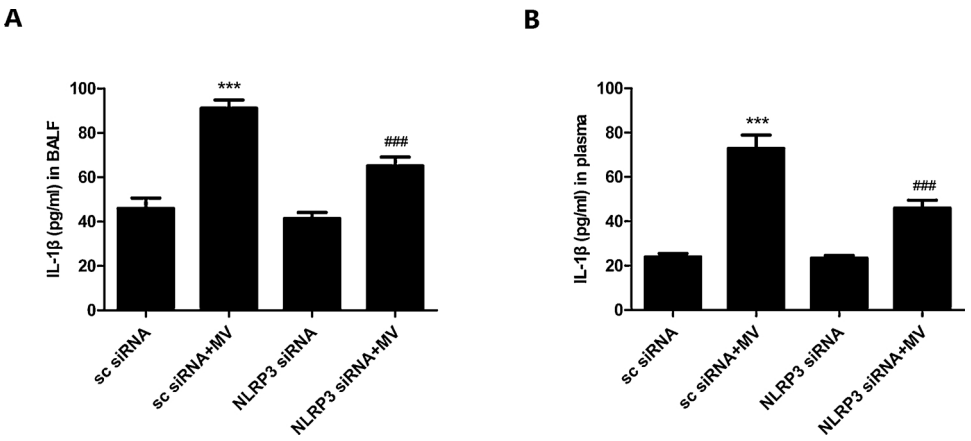

Fig. 6. NLRP3 decreased the secretion of IL-1β in vivo under mechanical ventilation. The levels of IL-1β in BALF **(A)** and in plasma **(B)** were detected by ELISAs. All the experiments were repeated at least three times. $^{***}p < 0.001$ versus the sc siRNA group, $^{\#\#\#}p < 0.001$ versus the sc siRNA + MV group.

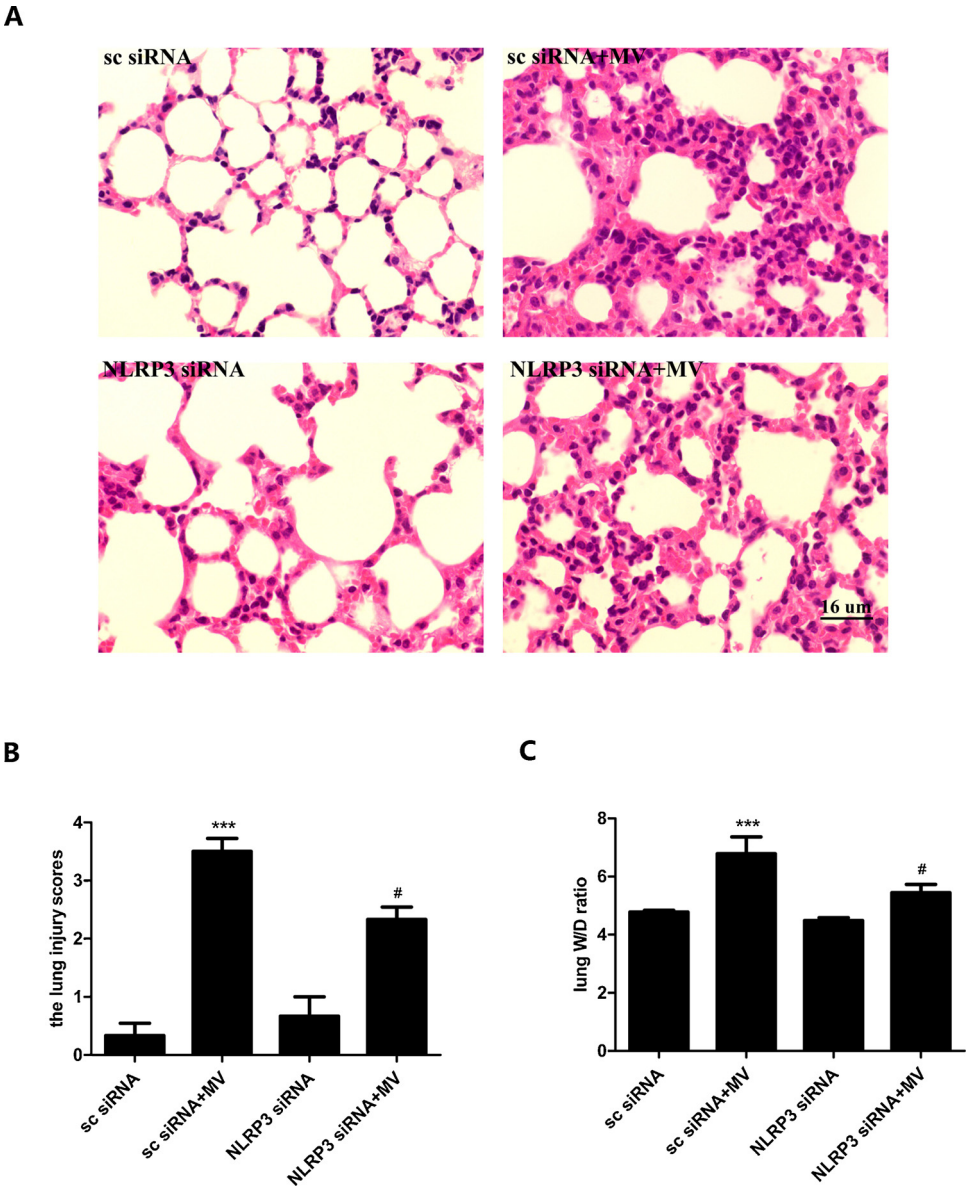

Fig. 7. Effects of NLRP3 on ventilator-induced lung injury. (A) The pathological changes of lung tissues were determined by H−E staining (magnification 400×), the scale bar was 16 μm. **(B)** Lung injury scores were applied to evaluate the severity of lung injury in different groups. $^{***}p < 0.001$ versus the sc siRNA group, $^{\#}p < 0.05$ versus the sc siRNA + MV group. **(C)** The degree of pulmonary edema was evaluated by the lung W/D ratio. We did at least three independent repeated experiments. $^{***}p < 0.001$ versus the sc siRNA group, $^{\#}p < 0.05$ versus the sc siRNA + MV group.

slides and subsequently incubated with anti-NEK7 (1:100) (Santa Cruz, USA), anti-NLRP3 (1:100) (Abcam, UK), anti-p120 (1:100) (Santa Cruz, USA), anti-E-cadherin (1:200) (Santa Cruz, USA), anti-ASC (1:100) (Santa Cruz, USA) and anti-caspase-1 (1:100) (Santa Cruz, USA) antibodies diluted in 5% BSA overnight at 4 °C. The specimens were then incubated with appropriate green and red fluorescent secondary antibodies at room temperature for an hour. The nuclei were dyed with 4′,6-diamidino-2-phenyl indole dihydrochloride (DAPI) for 5 min, after which the cells and frozen sections were rinsed four times with PBS. Next, antifade mounting medium was added to the glass slides to observe the colocalization of NLRP3, NEK7 and ASC, caspase-1 and p120, E-cadherin using a high sensitivity laser confocal microscope (Zeiss LSM 780, Carl Zeiss, Germany).

2.10. Statistical analysis

The experimental data are expressed as the mean ± standard deviation. One-way analysis of variance (ANOVA) and Bonferroni post hoc tests were used to analyze the significance of differences among all groups. When $p < 0.05$, the difference was considered statistically significant. All experimental data were analyzed using GraphPad Prism 5.0 software.

3. Results

3.1. NEK7 mediates the NLRP3 inflammasome activation after cyclic stretching

To explore the effects of cyclic stretching on NEK7/NLRP3 inflammasome activation, we detected the levels and colocalization of NEK7 and NLRP3; the combination of NLRP3, ASC, and procaspase-1; and the colocalization of ASC and caspase-1. All of these measures increased in a time-dependent manner after cyclic stretching compared with those of the control group (Fig. 1A-F), which indicated that the NLRP3 inflammasome could be activated by activating NEK7 after cyclic stretching in this procedure.

3.2. NLRP3 regulated the activation of the NLRP3 inflammasome as well as the degradation of cell junction proteins after cyclic stretching in MLE-12 cells

Immunoprecipitation was used to detect binding between ASC and procaspase-1. Western blotting was used to determine the expression of NLRP3 and cell junction proteins. The results suggested that the combination was decreased in the group that NLRP3 siRNA treated with cyclic stretch compared with the sc siRNA and cyclic stretch-treated group, which indicated that NLRP3 was the main factor for NLRP3 inflammasome activation. Additionally, cyclic stretch caused the degradation of p120 and occludin ($p < 0.001$). However, the degradation of cell junction proteins was alleviated when we also exposed MLE-12 cells to 20% cyclic stretch for 4 h after NLRP3 depletion ($p < 0.001$) (Fig. 2A-E).

Immunofluorescence distinctly demonstrated the colocalization of p120 and E-cadherin after cyclic stretching in MLE-12 cells for 4 h. The expression and colocalization of these proteins were notably decreased, and the above adverse phenomena were mitigated despite the NLRP3 depletion with cyclic stretch (Fig. 2F). Hence, NLRP3 depletion inhibited the activation of the NLRP3 inflammasome and promoted the stability of cell junctions.

3.3. NLRP3 affected the changes in mitochondrial membrane potential induced by cyclic stretching

Structural damage and dysfunction are two aspects of mitochondrial damage; mitochondrial dysfunction decreases the mitochondrial membrane potential. We found that NLRP3 inflammasome activation was closely associated with mitochondrial activity. To explore the effects of the NLRP3 inflammasome on mitochondrial membrane potential, we used flow cytometry to analyze the changes. The results revealed that mitochondrial membrane potential significantly decreased after cyclic stretching ($p < 0.001$), while the decrease in mitochondrial membrane potential was reduced in the group that underwent NLRP3 depletion with cyclic stretch ($p < 0.05$) (Fig. 3A-B).

3.4. NLRP3 depletion suppressed the IL-1β secretion induced by cyclic stretching

Cyclic stretch activated the NLRP3 inflammasome, and the precursor IL-1β was finally converted to its active form and secreted. The IL-1β level in the cell supernatant was examined by ELISAs, as shown in Fig. 4. The level was significantly increased in the cyclic stretch group, while the increased level was attenuated in the group that NLRP3 depletion with cyclic stretch ($p < 0.001$, $p < 0.05$) (Fig. 4).

3.5. Role of NLRP3 in regulating ventilator-induced lung injury

To further corroborate our data in vivo, we used C57BL/6 mice to demonstrate the role of NLRP3 in VILI. Further experiments were carried out after NLRP3 depletion.

As shown in Fig. 5 (A–D), the expression levels of p120 and occludin were reduced after mechanical ventilation ($p < 0.001$), which was consistent with previous studies (Gu et al., 2015); however, the degradation of cell junction proteins was alleviated in the group that underwent NLRP3 depletion and mechanical ventilation ($p < 0.05$, $p < 0.01$). Furthermore, the colocalization of p120 and E-cadherin in lung tissues was also weakened in the sc siRNA + MV group, but the attenuated colocalization was repaired in the NLRP3 siRNA + MV group.

Moreover, the IL-1β levels in BALF and plasma were increased remarkably after mechanical ventilation, but the increase was mitigated in the group that underwent NLRP3 depletion with mechanical ventilation ($p < 0.001$) (Fig. 6A-B).

To directly observe lung injury, we used H-E staining to assess the pathological changes in lung tissues. As shown in Fig. 7A, the prominent features of the lung tissues in the mechanical ventilation group were destruction of the destroyed pulmonary architecture, thickened alveolar septa, hyaline membrane formation, alveolar hemorrhage and infiltration of inflammatory cell. However, only a few infiltrating inflammatory cells were found in the sc siRNA- and NLRP3 siRNA-treated groups, and the above phenomena were mitigated in the NLRP3 depletion with mechanical ventilation group. In addition, the lung injury scores in the different groups were consistent with the above results (Fig. 7B).

Pulmonary edema was evaluated via the lung W/D ratio. As shown in Fig. 7C, the lung W/D ratio increased dramatically in the mechanical ventilation group but mildly in the NLRP3 depletion with mechanical ventilation group compared with the sc siRNA and NLRP3 siRNA-treated group ($p < 0.001$, $p < 0.05$), which indicated that NLRP3 depletion could reduce vascular permeability and pulmonary edema in VILI (Fig. 7C).

4. Discussion

Mechanical ventilation induced the production of proinflammatory cytokines and inflammatory mediators, which may have a central role in the mechanism of lung inflammation and injury in VILI. NLRP3 could be activated under mechanical stretching by activating the TLR-4/NF-κB pathway. In this study, we also verified that cyclic stretch induced the activation of the NLRP3 inflammasome via activating NEK7, which is involved in mitosis; our results are consistent with the findings of other studies (Wu et al., 2013) (Fig. 1A-F). However, the above phenomena were alleviated when we applied mechanical stretch to NLRP3-

depleted cells (Fig. 2A). Our results suggest that NLRP3 is crucial for regulating the assembly and activation of the NLRP3 inflammasome.

Adherens and tight junction proteins play a leading role in maintaining normal alveolar permeability (Ozaki et al., 2010; Luo et al., 2018). Mechanical stretch induced the degradation of adherens and tight junction proteins and reduced the colocalization of p120 and E-cadherin; however, the degradation of cell junction proteins was decreased in the groups that underwent NLRP3 depletion with mechanical stretch both in vitro and in vivo (Figs. 2B-F and 5 A, C-E). We speculate on the basis of these results that NLRP3 inflammasome activation is an important factor in destroying cell junctions, thereby increasing vascular permeability in VILI. The relationships between and among NLRP3, cell junction proteins and the increased vascular permeability in VILI should be further studied.

Cyclic stretch caused changes in mitochondrial membrane potential, which maintained the energy metabolism and thus allowed cell junction proteins to be preserved (Yu and Lee, 2016). Therefore, we examined the changes that occurred after cyclic stretching. The results indicated that the mitochondrial membrane potential decreased in the cyclic stretch group, while the decrease was alleviated in the NLRP3 depletion with cyclic stretch group (Fig. 3A-B). Thus, NLRP3 inflammasome activation might induce a decrease in mitochondrial membrane potential, which was the main reason for the degradation of cell junction proteins.

As previously shown, the secretion of IL-1β under mechanical stretching was dependent on the activation of the NLRP3 inflammasome (Wu et al., 2013). In this study, we detected the combination of NLRP3, ASC and procaspase-1 to reflect the activation of the NLRP3 inflammasome (Zhu et al., 2018). The results suggested that mechanical stretch activated the NLRP3 inflammasome and increased the secretion of IL-1β both in vitro and in vivo; however, NLRP3 depletion with mechanical stretch inhibited the formation of the NLRP3 inflammasome and decreased the secretion of IL-1β (Coates et al., 2017), which emphasized the crucial role of NLRP3 inflammasome activation in mediating lung inflammation in VILI (Figs. 4 and 6A-B).

Pulmonary edema is the earliest manifestation of VILI, and its main causes are the destruction of alveolar membrane integrity and the decrease of cell junction proteins due to changes in the cellular structure and function induced by mechanical stretching, which further increase the permeability of the pulmonary vascular barrier and the exudation of edema fluid along with dissolved albumin. In this study, we evaluated the lung W/D ratio to describe the extent of pulmonary edema in an in vivo mouse model of VILI. NLRP3 depletion decreased the lung W/D ratio and mitigated the pathological changes in lung tissues after mechanical ventilation, demonstrating the regulatory role of NLRP3 in VILI (Fig. 7A-C).

Our study revealed that mechanical stretch induced the activation of the NLRP3 inflammasome by activating NEK7; furthermore, we found that NLRP3 inflammasome activation could mediate the release of cytokines and the degradation of cell junction proteins and induce a decrease in mitochondrial membrane potential. This study verified that VILI could be alleviated by inhibiting the activation of the NLRP3 inflammasome, providing a new target for the prevention and treatment of VILI in the clinic.

Authors' contributions

All authors read and approved the final manuscript. YW and CG designed the research; HL performed experiments and prepared figures; HL, CG and YW edited and revised manuscript; ML, GL, DW and XL analyzed data.

Ethics approval and consent to participate

This study were approved by the Animal Ethics Committee of Qianfoshan Hospital of Shandong University.

Competing interests

The authors declare that they have no competing interests.

Acknowledgements

We were genuinely grateful to Medical Research Center of Qianfoshan Hospital of Shandong University for providing technical support for this study.

Funding

Our study was supported by National Natural Science Foundation (No. 81570074/H0111, No. 81770076/H0111), the Youth Foundation of National Natural Science Foundation (No. 81600054/H0111), Shandong Taishan Scholars and Young Experts Program and the Joint Project of Shandong Natural Science Foundation (No. ZR2015HL002) of China.

References

Babelova, A., Moreth, K., Tsalastra-Greul, W., Zeng-Brouwers, J., Eickelberg, O., et al., 2009. Biglycan, a danger signal that activates the NLRP3 inflammasome via toll-like and P2X receptors. J. Biol. Chem. 284, 24035–24048.
Blank, R., Napolitano, L.M., 2011. Epidemiology of ARDS and ALI. Crit. Care Clin. 27, 439–458.
Cannizzaro, V., Hantos, Z., Sly, P.D., Zosky, G.R., 2011. Linking lung function and inflammatory responses in ventilator-induced lung injury. Am. J. Physiol. Lung Cell Mol. Physiol. 300, L112–120.
Coates, B.M., Staricha, K.L., Ravindran, N., Koch, C.M., Cheng, Y., Davis, J.M., Shumaker, D.K., Ridge, K.M., 2017. Inhibition of the NOD-Like receptor protein 3 inflammasome is protective in juvenile influenza a virus infection. Front. Immunol. 8, 782.
Gasse, P., Riteau, N., Charron, S., Girre, S., Fick, L., et al., 2009. Uric acid is a danger signal activating NALP3 inflammasome in lung injury inflammation and fibrosis. Am. J. Respir. Crit. Care Med. 179, 903–913.
Gattinoni, L., Tonetti, T., Cressoni, M., Cadringher, P., Herrmann, P., et al., 2016. Ventilator-related causes of lung injury: the mechanical power. Intensive Care Med. 42, 1567–1575.
Gov, L., Schneider, C.A., Lima, T.S., Pandori, W., Lodoen, M.B., 2017. NLRP3 and potassium efflux drive rapid IL-1beta release from primary human monocytes during toxoplasma gondii infection. J. Immunol. 199, 2855–2864.
Gu, C., Liu, M., Zhao, T., Wang, D., Wang, Y., 2015. Protective role of p120-catenin in maintaining the integrity of adherens and tight junctions in ventilator-induced lung injury. Respir. Res. 16, 58.
Gudmundsson, M., Perchiazzi, G., Pellegrini, M., Vena, A., Hedenstierna, G., Rylander, C., 2018. Atelectasis is inversely proportional to transpulmonary pressure during weaning from ventilator support in a large animal model. Acta Anaesthesiol. Scand. 62, 94–104.
Han, S., Lear, T.B., Jerome, J.A., Rajbhandari, S., Snavely, C.A., et al., 2015. Lipopolysaccharide primes the NALP3 inflammasome by inhibiting its ubiquitination and degradation mediated by the SCFFBXL2 E3 ligase. J. Biol. Chem. 290, 18124–18133.
Hess, D.R., Kallstrom, T.J., Mottram, C.D., Myers, T.R., Sorenson, H.M., et al., 2003. Care of the ventilator circuit and its relation to ventilator-associated pneumonia. Respir. Care 48, 869–879.
Hoffman, H.M., Wanderer, A.A., 2010. Inflammasome and IL-1beta-mediated disorders. Curr. Allergy Asthma Rep. 10, 229–235.
Jain, S.V., Kollisch-Singule, M., Satalin, J., Searles, Q., Dombert, L., et al., 2017. The role of high airway pressure and dynamic strain on ventilator-induced lung injury in a heterogeneous acute lung injury model. Intensive Care Med. Exp. 5, 25.
Keszler, M., 2005. Volume-targeted ventilation. J. Perinatol. 25 (Suppl 2), S19–22.
Kuipers, M.T., Aslami, H.J., Janczy, R., Vander Sluijs, K.F., Vlaar, A.P., et al., 2012. Ventilator-induced lung injury is mediated by the NLRP3 inflammasome. Anesthesiolog 116, 1104–1115.
Lee, S., Suh, G.Y., Ryter, S.W., Choi, A.M., 2016. Regulation and function of the nucleotide binding domain leucine-rich repeat-containing receptor, pyrin Domain-Containing-3 inflammasome in lung disease. Am. J. Respir. Cell Mol. Biol. 54, 151–160.
Lewandowski, K., 1999. Epidemiological data challenge ARDS/ALI definition. Intensive Care Med. 25, 884–886.
Liu, Q., Lv, H., Wen, Z., Ci, X., Peng, L., 2017. Isoliquiritigenin activates nuclear factor Erythroid-2 related factor 2 to suppress the NOD-Like receptor protein 3 inflammasome and inhibits the NF-kappaB pathway in macrophages and in acute lung injury. Front. Immunol. 8, 1518.
Luo, W.W., Wang, X.W., Ma, R., Chi, F.L., Chen, P., Cong, N., Gu, Y.Y., Ren, D.D., Yang, J.M., 2018. Junctional E-cadherin/p120-catenin is correlated with the absence of supporting cells to hair cells conversion in postnatal mice cochleae. Front. Mol. Neurosci. 11, 20.
Ozaki, C., Yoshioka, M., Tominaga, S., Osaka, Y., Obata, S., et al., 2010. p120-Catenin is

essential for N-cadherin-mediated formation of proper junctional structure, thereby establishing cell polarity in epithelial cells. Cell Struct. Funct. 35, 81–94.
Seiberlich, E., Santana, J.A., Chaves, Rd.A., Seiberlich, R.C., 2011. Protective mechanical ventilation, why use it? Braz. J. Anesthesiol. 61, 659–667.
Wang, Y., Minshall, R.D., Schwartz, D.E., Hu, G., 2011. Cyclic stretch induces alveolar epithelial barrier dysfunction via calpain-mediated degradation of p120-catenin. Am. J. Physiol. Lung Cell Mol. Physiol. 301, L197–206.
Wu, J., Yan, Z., Schwartz, D.E., Yu, J., Malik, A.B., Hu, G., 2013. Activation of NLRP3 inflammasome in alveolar macrophages contributes to mechanical stretch-induced lung inflammation and injury. J. Immunol. 190, 3590–3599.
Xi, H., Zhang, Y., Xu, Y., Yang, W.Y., Jiang, X., et al., 2016. Caspase-1 inflammasome activation mediates homocysteine-induced pyrop-apoptosis in endothelial cells. Circ. Res. 118, 1525–1539.
Xu, J.F., Washko, G.R., Nakahira, K., Hatabu, H., Patel, A.S., et al., 2012. Statins and pulmonary fibrosis: the potential role of NLRP3 inflammasome activation. Am. J. Respir. Crit. Care Med. 185, 547–556.
Yadam, S., Bihler, E., Balaan, M., 2016. Acute respiratory distress syndrome. Crit. Care Nurs. Q. 39, 190–195.
Yu, J.W., Lee, M.S., 2016. Mitochondria and the NLRP3 inflammasome: physiological and pathological relevance. Arch. Pharm. Res. 39, 1503–1518.
Zhang, Q., Wu, D., Yang, Y., Liu, T., Liu, H., 2017. Dexmedetomidine alleviates hyperoxia-induced acute lung injury via inhibiting NLRP3 inflammasome activation. Cell. Physiol. Biochem. 42, 1907–1919.
Zhao, T., Liu, M., Gu, C., Wang, X., Wang, Y., 2014. Activation of c-Src tyrosine kinase mediated the degradation of occludin in ventilator-induced lung injury. Respir. Res. 15, 158.
Zhu, J., Hu, Z., Han, X., Wang, D., Jiang, Q., et al., 2018. Dopamine D2 receptor restricts astrocytic NLRP3 inflammasome activation via enhancing the interaction of beta-arrestin2 and NLRP3. Cell Death Differ.